PDF analysis of ferrihydrite: Critical assessment of the underconstrained akdalaite model

A. Manceau, S. Skanthakumar, L. Soderholm

PDF analysis of ferrihydrite: Critical assessment of the underconstrained akdalaite model

A. Manceau[1,*] S. Skanthakumar[2] and L. Soderholm[2]

[1]ISTerre, CNRS and Université de Grenoble 1, 38041 Grenoble Cedex 9, France.
[2]Chemical Sciences and Engineering Division, Argonne National Laboratory, CHM/200, 9700 S. Cass Avenue, Argonne, IL 60439, USA.

* To whom correspondence should be addressed. E-mail: Alain.Manceau@ujf-grenoble.fr
Running title : PDF analysis of ferrihydrite
Keywords: structure, ferrihydrite, pair distribution function, PDF, HEXS,

ABSTRACT

In an effort to shed light on the intricate structure of ferrihydrite, its pair distribution function (PDF) derived from high-energy X-ray scattering (HEXS) data was refined with the single-phase akdalaite model, possessing 20% of the Fe atoms in tetrahedral coordination, and a modified akdalaite model in which Fe has only octahedral coordination. The second model is analogous to the predominant f-phase (ABAC stacking sequence) of classical multi-phase ferrihydrite. The contribution from the disordered d-phase component (randomly stacked ABA and ACA double-layer fragments) of the classical model was recovered in the modified akdalaite description by increasing the atomic motion of the ABAC motif above the double-layer distance 4.2 Å to simulate aperiodic stacking faults. Results show that the original and modified akdalaite representations provide near-identical fits to the ferrihydrite PDF. In the original single-phase and periodic model, the plurality of the Fe-O and Fe-Fe distances resulting from phase mixtures and defects are reconciled artificially by taking a large unit–cell with three independent Fe sites, two Fe coordinations, and underconstrained atomic positions. Correlation matrices reveal that many fitted parameters are linearly correlated, thus explaining the crystallographic and chemical inconsistencies of the as-refined akdalaite model which have been identified in the literature. Structurally more constrained, the modified akdalaite model does not suffer from bias and provides a more robust description of the PDF data. However, because structural defects and inhomogeneities are not physically present but introduced artificially in PDF modeling, the crystallographic description of ferrihydrite by real-space modeling of HEXS data has an idealized character. To facilitate further understanding of the ferrihydrite structure, the PDF data are provided as supplementary material for interlaboratory testing, and as a resource as more sophisticated tools may be brought to bear on this complex problem.

INTRODUCTION

Ferrihydrite (Fh), of average composition $FeOOH \cdot 0.2\text{-}0.4H_2O$ (Rancourt and Meunier, 2008; Hiemstra and Van Riemsdijk, 2009), is the most common iron oxyhydroxide in soils, oxidized sediments and mine wastes, the main iron-rich core of the ferritin protein present in all kingdoms of life, and a likely constituent in extraterrestrial materials (Cowley et al., 2000; Fortin and Langley, 2005; Farrand et al., 2009; Theil et al., 2013). It is also a key reactive nanoparticle that regulates nutrient availability, the mobility of metal(loid)s contaminants such as arsenic, and an efficient catalyst of the degradation of organic polluants and H_2O_2 decomposition (Jambor and Dutrizac, 1998; Cornell and Schwertmann, 2003; Ma et al., 2012). Although ferrihydrite is critical to numerous geochemical and biological processes, and a material of choice in technological and industrial applications, its atomic structure has remained a point of speculation. Five structural models have been proposed over the years (Harrison and al., 1967; Towe and Bradley, 1967; Eggleton and Fitzpatrick, 1988; Drits et al., 1993; Michel et al., 2007); the first three have been invalidated (Drits et al., 1993), and the two most recent only partly accepted, because neither of them satisfactorily describe all X-ray, electron and neutron diffraction, and spectroscopic data. The two competing structural descriptions are expressed as the 'Drits model', which is multi-phase, and the 'Michel model', which is single-phase and isostructural to akdalaite ($^{VI}Al_8{}^{IV}Al_2O_{14}(OH)_2$; Fig. 1) (Drits et al., 1993; Michel et al., 2007).

The Drits multi-phasic model was derived from powder X-ray diffraction data. It is composed dominantly of the "f-phase" ($FeO_{0.85}OH$) mixed with lesser amounts of the "d-phase" (FeOOH) and nanocrystalline hematite (α-Fe_2O_3). The f-phase consists of oxygen and hydroxyl sheets stacked in an ABAC packing sequence along the *c* direction, and Fe atoms which occupy at random 50% of the octahedral sites in each anionic layer (Fig. 1a). The d-phase is a disordered feroxyhite (δ-FeOOH) and consists of ABA and ACA double-layer fragments randomly stacked. The three components of the Drits model have been observed using high-resolution transmission electron microscopy (HRTEM), including single-crystal electron nanodiffraction (Cowley et al., 2000; Janney et al., 2000, 2001). The feroxyhite-type local structure of the d-phase was described in terms of a "double chain structure" by Janney et al. (2000), but in reality this structural component is the same as the d-phase (Manceau, 2009). The alternative akdalaite model for ferrihydrite was derived from the pair distribution function (PDF) analysis of high-energy X-ray and neutron scattering data (Michel et al., 2007). It has the same ABAC stacking sequence as the f-phase, but differs from it by 20% Fe occupancy of the tetrahedral sites and 80% Fe occupancy of the octahedral sites and fewer OH groups (Fig. 1b).

The Drits model accounts for all available chemical, structural and spectroscopic data except the PDF, which does not fit well. In addition, it predicts that ferrihydrite containing ordered feroxyhite fragments would have seven diffraction lines (7Fh), not six (6Fh) as commonly observed for natural and synthetic crystalline ferrihydrite (Jambor and Dutrizac, 1998; Cornell and Schwertmann, 2003). This prediction has been verified recently with the successful synthesis of a well-crystallized seven-line ferrihydrite (Fig. 2) (Berquo et al., 2007). In contrast to the Drits model, the akdalaite model reproduces the PDF for both highly defective two-line ferrihydrite (2Fh) and crystalline six-line ferrihydrite (6Fh), but is inconsistent with other experimental observations (Manceau and Gates, 2013). Two important shortcomings of the akdalaite structure are the failure

to reproduce the X-ray diffraction (XRD) pattern of 6Fh and 7Fh (Fig. 2) (Rancourt and Meunier, 2008; Manceau, 2012), and the lack of evidence for tetrahedral Fe, as reported in the most diagnostic spectroscopic study to date (Paktunc et al., 2013). Because the akdalaite model entirely relies on the interpretation of the ferrihydrite PDF, results warrant further examination.

In PDF analyses, a structural model is assumed and its unit cell dimensions and atomic coordinates regressed against the experimental data under the symmetry constraints of a space group (Billinge and Kanatzidis, 2004; Neder and Korsunskiy, 2005; Farrow et al., 2007; Proffen and Kim, 2009). As powerful as this method is, its applicability for the resolution of the average structure of defective and multi-component nanomaterials is intrinsically limited by the presumption of a unit cell repeated in three dimensions. If defects are ordered, they can be described with proper models using a supercell. In the case of aperiodic stacking fault with low probability, modeling still is possible, although in an approximate way, by introducing anisotropic atomic displacements (*i.e.*, *U* parameter) in the stacking direction (Petkov et al., 2002; Masadeh et al., 2007). Here, these two approaches are deceptive because ferrihydrite is a mixture of nanoparticles with different structures, shape, domain size, point defects, and stacking disorder, and also has randomness. Clearly, its structure is too complex to be captured realistically by PDF with a simple physical description, as is the case also for nanostructured and defect phyllomanganates (Manceau et al., 2013). This difficulty raises questions about the reason why the periodic akdalaite structure provides a good fit to PDF. We show that the large range of interatomic distances and bond angles, typical of Fh, is reconciled in the akdalaite fit with an apparently unfaulted average structure by employing a large unit–cell with three independent Fe sites and under-constrained atomic positions. The demonstration is carried out through comparison of the best-fit calculations obtained, (1) with the original akdalaite model, in which two Fe are octahedral and one tetrahedral (Fig. 1b), and (2) a modified akdalaite model in which Fe is fully octahedral with 50% occupancy (Fig. 1c).

EXPERIMENTAL METHOD AND DATA REDUCTION

The PDF of the 6Fh sample used to derive the Drits model (Fig. 1a) was measured at the Advanced Photon Source (APS) on beamline 11-ID-B with an X-ray energy of 90.480 keV (λ= 0.13702 Å). For consistency quality of the results, the total X-ray scattering data used to calculate the PDF was acquired on the same instrument as the one used to derive the akdalaite model (Michel et al., 2007). The total scattering structure function, $S(q)$, was obtained as described previously (Soderholm et al., 2005; Skanthakumar and Soderholm, 2006), and the PDF was calculated by integration of the reduced structure function $F(q)$ (Egami and Billinge, 2003; Billinge and Kanatzidis, 2004) over the $0.5 \leq q \leq 21$ Å^{-1} interval. The PDF data are provided as Supplementary material for interlaboratory testing and as a resource for further analysis with more sophisticated tools.

RESULTS

Simulation of the ferrihydrite PDF with tetrahedral and octahedral Fe

The PDFs for the six-line ferrihydrites of Michel (fhyd6) and Drits (6Fh) are essentially identical (Fig. 3a,b). The positions and relative intensities of the PDF peaks are in close proximity out to r_{max} = 20 Å, indicating that the two nanomaterials have about the same domain size. The first peak at r = 1.99 Å is from the Fe-(O,OH,H_2O) pairs, and the next two at r ~ 3.0 Å and 3.4-3.5 Å dominantly from the Fe-Fe distances across shared-edges and shared-corners (Fig. 1a).

Lattice constants and atomic positions were refined in the same space group ($P6_3mc$) using the same least-squares PDF-profile fitting program (PDFgui 1.0) (Farrow et al., 2007) as Michel et al. (2007). The structure of the model and its parametrization in PDFgui are shown in Supplementary Figure 1. A main criticism of the 2007 refinement (fhyd6) has been its failure to satisfy the bond valence sums of cations and anions, in violation of Pauling's 2nd rule (Table 1) (Manceau, 2009). This inconsistency was corrected in 2010 with a new refinement (ferrifh) (Michel et al., 2010), but at the expense of introducing strong distortions in violation of Pauling's distortion rule (Table 2) (Manceau, 2011). Twenty parameters were allowed to vary in the fhyd6 refinement and nineteen in the ferrifh refinement. Adjusting the 6Fh PDF with twenty or nineteen parameters, similar to the fit strategy adopted for the fhyd6 and ferrifh refinements, produced near-identical agreement factors (R_w = 28.5 % vs. 27.0 %; Supplementary Tables 1 and 2), and the same fit quality as the akdalaite model (R_w = 26.7 %; Fig. 3a,b). The new atomic coordinates and unit cell parameters coincide with those reported previously. Electrical charges are also unbalanced and the Fe polyhedra strongly distorted in the new simulation (Tables 1,2). The polyhedral representations of the two refined structures show that some Fe octahedra are anomalously elongated and the tetrahedral Fe atom excessively off-centered and unrealistically close to one tetrahedral face (Fig. 1b), consistent with previous observations for fhyd6 (Manceau, 2009).

Parameter correlations, which are not reported in Michel et al. (2007), show that many fitted parameters are linearly correlated (ρ = 1) when twenty variables are refined simultaneously (Supplementary Table 1). Fixing the ^{VI}Fe1 site occupancy to 1.0 suppresses almost all correlations, except the ^{VI}Fe2 and ^{IV}Fe3 occupancies, which remain severely anti-correlated (ρ = -0.87; Supplementary Table 2). This result casts doubt on the accuracy of the precision reported in the previous refinements. High correlations between atomic coordinates mean that some atoms can be moved in one direction and others in another with no significant change in quality of the fit to the PDF. For example, constraining the model to satisfy Pauling's bond valence sum introduces, or reinforces, other structural irregularities, such as the violation of Pauling's distortion rule (Tables 1,2). One reason for model bias is the impossibility to define upper and lower bounds for the adjusted values in PDFgui, causing some parameters to take unrealistic values and to be correlated if the refinement is under-constrained (Supplementary Tables 1 and 2). The akdalaite model has more adjustable parameters than independent data points in the PDF. The PDF fitting software seeks structural solutions in a deep flat-bottomed valley with countless "local" minima, and so will always find the best "local" solution that it can, which is highly dependent on the initial parametrization. Actually, modelers are cautioned against the risk of overfitting PDF data in the PDFFIT User Guide: ''The problem of determining the structure of a nanoparticle remains difficult.

PDFgui is not intended to necessarily provide *the* solution; it is rather a helpful tool in the process of determining new details and exploring the space of possible solution candidates, yielding success in some instances'' (Farrow et al., 2007).

Simulation of the ferrihydrite PDF with octahedral Fe

The co-existence in the Drits model of the f-phase, d-phase, and nanohematite with different space groups ($P\bar{3}1c$, $P\bar{3}m1$, and $R\bar{3}c$, respectively) makes the PDF parametrization difficult. In addition, the multi-component model has four Fe positions and four O positions; clearly the data lack sensitivity to quantify the full distribution of all generated atomic pairs. As a first approximation, the problem can be simplified by omitting contributions from the minor d-phase and nanohematite. Also, the d-phase is too disordered to produce a signal at intermediate to long distances (r > ~5 Å). Another source of complication is that the PDF sees the short- to long-range structure of the f-phase, which deviates from the Bragg-average structure derived from diffraction. The f-phase was refined with only one crystallographic parameter, the z position of Fe. Its asymmetric unit contains one Fe in the 4f position (1/3, 2/3, z) and two O atoms at the special positions of undeformed ABAC close packing. Therefore, the eight octahedra from the 2x2x1 supercell represented in Figure 1c are all equivalent in the Drits model, and have only two Fe-O distances. Clearly, this model is now over-constrained and its symmetry needs to be lowered to fit the PDF. In comparison, the asymmetric unit of the akdalaite structure has three Fe (two ^{VI}Fe and one ^{IV}Fe) and four O atoms, resulting in eight Fe-O distances and 10 independent crystallographic positions refined in the PDF analysis (Supplementary material).

A f-phase model suitable for PDF refinement can be derived from the akdalaite structure with the following changes and constraints: (1) the ^{IV}Fe position is unoccupied; (2) one of the three ^{VI}Fe atoms in the AB and AC layers are moved to the adjacent BA and CA layers to satisfy the 50% occupancy of each anion layer in the f-phase; (3) the distribution of Fe across the anion layers is such that there are no face-sharing arrangements between Fe octahedra along the B and C planes of the structure (Fig. 1c, Supplementary Fig. 2). The modified akdalaite model also has 10 independent crystallographic positions (3 ^{VI}Fe + 4 O positions), but a narrower distribution of the Fe-O and Fe-Fe distances because Fe has only one coordination (^{VI}Fe) vs. two in the original akdalaite model (^{VI}Fe + ^{IV}Fe).

Correlated atomic motion was accounted for differently in the fits of the original and modified akdalaite models to the 6Fh PDF. The motion of the two contributing atoms in an atomic pair is uncorrelated at large distance, but correlated when their distance separation is small (Jeong et al., 2003). This effect sharpens the first peaks in the observed PDF. The radial dependence of this effect on the PDF peak width (σ_{ij}) usually is described with a *delta*/r or *delta*/r^2 function, as was the case for the original akdalaite model. The analytical expression implemented in PDFgui is:

$$\sigma_{ij} = \sigma'_{ij}\sqrt{1-\frac{\delta_1}{r_{ij}}-\frac{\delta_2}{r_{ij}^2}+Q_{broad}^2 r_{ij}^2}$$

where σ' is the peak width without correlation, calculated from the U values of the (an)isotropic displacement parameter (Supplementary material), and Q_{broad} is the experimental broadening. However, a continuous *delta* function may not be the most appropriate term to account for the loss

of structural coherence caused by stacking faults, especially if they occur at some specific distance separations, as the randomness of the ABA and ACA double-layer fragments from the d-phase would suggest. This inference is supported by the comparison of the PDFs from phyllomanganates (Fig. 4) (Manceau et al., 2013). The KBi8 and AcidBir layer manganates have the same structural formula and short-range layer structure, but a different density of stacking faults along the layer stack. The most *c*-disordered material (AcidBir) shows a discontinuity in peak intensity at distances greater than the interslab separation of 7.2 Å. A more extreme case is δ-MnO_2, in which the MnO_2 layers are randomly stacked. The loss of structural coherence in the *c* direction beyond 7.2 Å is manifested in the PDF as a sharp decrease in peak intensity beyond this distance (Fig. 4b). This type of disorder cannot be modeled with a *delta* function (Manceau et al., 2013).

Simulations of the 6Fh PDF with a *delta* function to test a similar effect in ferrihydrite resulted in a significant amplitude mismatch between experiment and theory beyond r = 4.5 Å. Here, the loss of structural coherence occurs on a length scale corresponding to the separation between two next-nearest O/OH sheets, *i.e.*, to the thickness of a double-layer fragment. This effect on the PDF can be accounted for empirically by defining a low-r to high-r PDF peak ratio with a cutoff value of 4.5 Å. The value of the peak ratio, which depends on the density of stacking faults, was optimized in the refinement with the fit parameter *sratio* replacing the *delta* function. The fit to the modified akdalaite model with nineteen parameters returned an R_w value of 32.7 %, which is about 20% higher than the best-fit value obtained with the original akdalaite model (Fig. 3, Supplementary Table 3). Does it mean that the modified model is less reasonable? We contend instead that it provides a more realistic description of the data based on the following considerations.

First, comparing the two theoretical PDFs (Fig. 3c), we see that they are nearly identical, meaning that the two models indistinctly capture the short- and longer-range correlations of the ferrihydrite PDF. The small difference of amplitude at 4.7 Å is related to how stacking faults are captured empirically in the two refinements.

Second, a two-site occupation model (^{VI}Fe + ^{IV}Fe) is expected to yield a better fit than a one-site model (^{VI}Fe). However, the difference between the two fits is marginal, and therefore insignificant given that structural defects and variability are not physically present but introduced artificially in the two models.

Third, correlations between parameters are all lower than 0.8 in the modified akdalaite model (Supplementary Table 3). Although somewhat arbitrary, this value corresponds to the hard-coded PDFgui threshold below which the refinement parameters are considered independent. Therefore, although the quality of the PDF fit improves when Fe is octahedral and tetrahedral, parameters are correlated (Supplementary Tables 1 and 2) indicating that the robustness of the modified akdalaite model in fact is improved relative to the original two-site model. Although the optimized one-site model is statistically more robust, the structure remains strongly distorted; the real sample is more complicated and cannot be assumed to be single-phase. This distortion is evaluated in Table 2 with the eccentricity Δ parameter, which measures the distance between the centroid of the Fe polyhedron and the central Fe atom, and the volume eccentricity, which describes the volume distortion of the polyhedron (Balic-Zunic and Makovicky, 1996; Balic-Zunic, 2007). The larger the eccentricity, the more a polyhedron deviates from the ideal.

Fourth, and most compelling, a comparison of the first PDF peaks for 6Fh and the crystalline phyllomanganate KBi8, used as a reference for octahedral Mn coordinated to 6O at 1.91 Å (Gaillot et al., 2003), shows that Fe is fully octahedral in ferrihydrite, similar to Mn in KBi8 (Fig. 5). The two metal-oxygen peaks are symmetrical, and the Fe-O peak broader than the Mn-O peak because the Fe atoms are bonded to three types of ligands, O, OH and H_2O, in various polyhedral associations. If 20% of the Fe atoms were tetrahedrally coordinated, as in the original akdalaite model, the distribution of the Fe-(O,OH,H_2O) distances would be asymmetric and the PDF peak broadened to lower *r*-values relative to the KBi8 peak.

To date, there is a consensus that the main structural component of six-line ferrihydrite has a hexagonal ABAC layer stacking sequence. A main difference between the Drits and Michel models is the site occupation of Fe, which is fully octahedral in the first model, and octahedral and tetrahedral in the second model. We showed that introducing three Fe sites and two Fe coordinations, as in the Michel model, slightly improves the match to PDF data, but decreases confidence in the results.

CONCLUDING REMARKS

The PDF method was originally a tool for studying amorphous bulk materials like glasses, liquids, and solutions (Waseda, 1980; Magini et al., 1988; Fischer et al., 2006), and short-range ordered inorganic materials (Billinge et al., 2005), to less than ~10 Å. Using this technique to determine the average structure of defective nanocrystals from full-pattern fitting of PDF decreases the sensitivity to details of the local structure, as reported recently for disordered phyllomanganates (Manceau et al., 2013). Similar issues were encountered in the analysis of biogenic MnO_x produced by freshwater *Acremonium sp.* fungi. Incorrect *a priori* model assumption led to conclude that this material has a todorokite-type three-dimensional tunnel structure (Petkov et al., 2009), when in reality the structure is two-dimensional (Grangeon et al., 2010). Therefore, PDF is of great value in determining the local atomic structure of materials, but can be biased for the average structure analysis of defective and multi-component materials because structural imperfections and heterogeneities are difficult to implement analytically. If caution is not exercised, multiple solutions may occur not only within a given model, but also among different models. For these types of materials, physically based models are easier to fit to HEXS data in reciprocal-space using Bragg analyses and the Debye equation (Fernandez-Martinez et al., 2010; Manceau et al., 2013).

ACKNOWLEDGEMENTS

The work at Argonne National Laboratory was supported by the U.S. Department of Energy, OBES, under contract number DE-AC02-06CH11357.

REFERENCES CITED

Balic-Zunic, T. (2007) Use of the three-dimensional parameters in the analysis of crystal structures under compression. In A. Grzechnik, Ed. Pressure Induced Phase Transitions. Transworld Research Network, Kerala, India.

Balic-Zunic, T. and Makovicky, E. (1996) Determination of the centroid or 'the best centre' of a coordination polyhedra. Acta Crystallographica B, 52, 78-81.

Berquo, T.S., Banerjee, S.K., Ford, R.G., Penn, R.L., and Pichler, T. (2007) High crystallinity Si-ferrihydrite: An insight into its Néel temperature and size dependence of magnetic properties. Journal of Geophysical Research, 112, B02102.

Billinge, S.J.L. and Kanatzidis, M.G. (2004) Beyond crystallography: the study of disorder, nanocrystallinity and crystallographically challenged materials with pair distribution functions. Chemical Communication, 7, 749-760.

Billinge, S.J.L., McKimmy, E.J., Shatnawi, M., Kim, H.J., Petkov, V., Wermeille, D., and Pinnavaia, T.J. (2005) Mercury binding sites in thiol-functionalized mesostructured silica. Journal of the America n Chemical Society, 127, 8492-8498.

Cornell, R.M. and Schwertmann, U. (2003) The Iron Oxides: Structure, Properties, Reactions, Occurrence and Uses. VCH verlag, Weinheim, Germany.

Cowley, J.M., Janney, D.E., Gerkin, R.C., and Buseck, P.R. (2000) The structure of ferritin cores determined by electron nanodiffraction. Journal of Structural Biology, 131, 210-216.

Drits, V.A., Sakharov, B.A., Salyn, A.L., and Manceau, A. (1993) Structural model for ferrihydrite. Clay Minerals, 28, 185-208.

Egami, T. and Billinge, S.J.L. (2003) Underneath the Bragg Peaks: Structural Analysis of Complex Materials. Pergamon, New York.

Eggleton, R.A. and Fitzpatrick, R.W. (1988) New data and a revised structural model for ferrihydrite. Clays and Clay Minerals, 36, 111-124.

Farrand, W.H., Glotch, T.D., Rice, J.W., Hurowitz, J.A., and Swayze, G.A. (2009) Discovery of jarosite within the Mawrth Vallis region of Mars: Implications for the geologic history of the region. ICARUS, 2004, 478–488.

Farrow, C.L., Juhas, P., Liu, J.W., Bryndin, D., Bozin, E.S., Bloch, J., Proffen, T., and Billinge, S.J.L. (2007) PDFfit2 and PDFgui: computer programs for studying nanostructure in crystals. Journal of Physics: Condensed Matter, 19, 335219.

Fernandez-Martinez, A., Timon, V., Roman-Ross, G., Cuello, G.J., Daniels, J.E., and Ayora, C. (2010) The structure of schwertmannite, a nanocrystalline iron oxyhydroxysulfate. Am. Miner., 95, 1312–1322.

Fischer, H.E., Barnes, A.C., and Salmon, P.S. (2006) Neutron and x-ray diffraction studies of liquids and glasses. Reports on Progress in Physics, 69, 233-299.

Fortin, D. and Langley, S. (2005) Formation and occurrence of biogenic iron-rich minerals. Earth-Science Reviews, 72, 1-19.

Gaillot, A.C., Flot, D., Drits, V.A., Burghammer, M., Manceau, A., and Lanson, B. (2003) Structure of synthetic K-rich birnessites obtained by high-temperature decomposition of KMnO4. I. Two-layer polytype from a 800°C experiment. Chemistry of Materials, 15, 4666-4678.

Grangeon, S., Lanson, B., Miyata, N., Tani, Y., and Manceau, A. (2010) Structure of nanocrystalline phyllomanganates produced by freshwater fungi. American Mineralogist, 95, 1608-1616.

Harrison, P.M., Fischbach, F.A., Hoy, T.G., and Haggis, G.H. (1967) Ferric oxyhydroxide core of ferritin. Nature, 216, 1188-1190.

Hiemstra, T. and Van Riemsdijk, W.H. (2009) A surface structural model for ferrihydrite I: Sites related to primary charge, molar mass, and mass density. Geochimica et Cosmochimica Acta, 73, 4423-4436.

Jambor, J.L. and Dutrizac, J.E. (1998) Occurrence and constitution of natural and synthetic ferrihydrite, a widespread iron oxyhydroxide. Chemical Reviews, 98, 2549-2585.

Janney, D.E., Cowley, J.M., and Buseck, P.R. (2000) Structure of synthetic 2-line ferrihydrite by electron nanodiffraction. American Mineralogist, 85, 1180-1187.

-. (2001) Structure of synthetic 6-line ferrihydrite by electron nanodiffraction. American Mineralogist, 86, 327-335.

Jeong, I.K., Heffner, R.H., Graf, M.J., and Billinge, S.J.L. (2003) Lattice dynamics and correlated atomic motion from the atomic pair distribution function. Physical Review B, 67, 104301.

Ma, Y., Meng, S., Qin, M., Liu, H.Z., and Wei, Y. (2012) New insight on kinetics of catalytic decomposition of hydrogen peroxide on ferrihydrite: Based on the preparation procedures of ferrihydrite Journal of Physics and Chemistry of Solids, 73, 30-34.

Magini, M., Licheri, G., Paschina, G., Piccaluga, G., and Pinna, G. (1988) X-ray diffraction of ions in aqueous solutions: hydration and complex formation. 267 p. CRC Press Inc., Boca Raton.

Manceau, A. (2009) Evaluation of the structural model for ferrihydrite derived from real-space modelling of high-energy X-ray diffraction data. Clay Minerals, 44, 19-34.

-. (2011) Critical evaluation of the revised akdalaite-model for ferrihydrite. American Mineralogist, 96, 521-533.

-. (2012) Critical evaluation of the revised akdalaite-model for ferrihydrite – Reply. American Mineralogist, 97, 255-256.

Manceau, A., and Gates, W.P. (2013) Incorporation of Al in ferrihydrite: Implications for the structure of ferrihydrite. Clay Minerals, 48, 481-489.

Manceau, A., Marcus, M.A., Grangeon, S., Lanson, M., Lanson, B., Gaillot, A.C., Skanthakumar, S., and Soderholm, L. (2013) Short-range and long-range order of phyllomanganate nanoparticles determined using high energy X-ray scattering. Journal of Applied Crystallography, 46, 193-209.

Masadeh, A.S., Bozin, E.Z., Farrow, C.L., Paglia, G., Juhas, P., Billinge, S.J.L., Karkamkar, A., and Kanatzidis, M.G. (2007) Quantitative size-dependent structure and strain determination of CdSe nanoparticles using atomic pair distribution function analysis. Physical Review B, 76, 115413.

Michel, F.M., Barrónc, V., Torrent, J., Moralesd, M.P., Sernad, C.J., Boilye, J.F., Liuf, Q., Ambrosinig, A., Cismasua, A.C., and Brown Jr., G.E. (2010) Ordered ferrimagnetic form of ferrihydrite reveals links among structure, composition, and magnetism. Proceedings of the National Academy of Science, 107, 2787–2792.

Michel, F.M., Ehm, L., Antao, S.M., Lee, P.L., Chupas, P.J., Liu, G., Strongin, D.R., Schoonen, M.A.A., Phillips, B.L., and Parise, J.B. (2007) The structure of ferrihydrite, a nanocrystalline material. Science, 316, 1726-1729.

Neder, R.B. and Korsunskiy, V.I. (2005) Structure of nanoparticles from powder diffraction data using the pair distribution function. Journal of Physics: Condensed Matter., 17, S125–S134.

Paktunc, D., Manceau, A., and Dutrizac, J. (2013) Incorporation of Ge in ferrihydrite: Implications for the structure of ferrihydrite. American Mineralogist, 98, 859-869.

Petkov, V., Ren, Y., Saratovsky, I., Pasten, P., Gurr, S.J., Hayward, M.A., Poeppelmeier, K.R., and Gaillard, J.F. (2009) Atomic-scale structure of biogenic materials by total X-ray diffraction: A study of bacterial and fungal MnO_x. ACS Nano, 3, 441-445.

Petkov, V., Trikalitis, P.N., Bozin, E.S., Billinge, S.J.L., Vogt, T., and Kanatzidis, M.G. (2002) Structure of $V_2O_5.nH_2O$ xerogel solved by the atomic pair distribution function technique. Journal of the American Chemical Society, 124, 10157-10162.

Post, J.E., Heaney, P.J., Von Dreele, R.B., and Hanson, J.C. (2003) Neutron and temperature-resolved synchrotron X-ray powder diffraction study of akaganéite. American Mineralogist, 88, 782-788.

Proffen, T. and Kim, H. (2009) Advances in total scattering analysis. Journal of Materials Chemistry, 19, 5078–5088.

Rancourt, D.G. and Meunier, J.F. (2008) Constraints on structural models of ferrihydrite as a nanocrystalline material. American Mineralogist, 93, 1412–1417.

Soderholm, L., Skanthakumar, S., and Neuefeind, J. (2005) Determination of actinide speciation in solution using high-energy X-ray scattering. Analytical and Bioanalytical Chemistry, 383, 48-55.

Skanthakumar, S. and Soderholm, L. (2006) Studying actinide correlations in solution using high-energy x-ray scattering. Materials Research Society Symposium Proceedings, 893, 411-416.

Theil, E.C., Behera, R.K., and Tosha, T. (2013) Ferritins for chemistry and for life. Coordination Chemistry Reviews, 257, 579-586.

Towe, K.M. and Bradley, W.F.J. (1967) Mineralogical constitution of colloidal "hydrous ferric oxides". Journal of Colloid and Interface Science, 24, 384-392.

Waseda, Y. (1980) The structure of non-crystalline materials. 326 p. McGraw-Hill Inc., New York.

Zhu, M., Farrow, C.L., Post, J.E., Livi, K.J.T., Billinge, S.J.L., Ginder-Vogel, M., and Sparks, D.L. (2012) Structural study of biotic and abiotic poorly-crystalline manganese oxides using atomic pair distribution function analysis. Geochimica et Cosmochimica Acta, 81, 39-55.

FIGURE CAPTIONS

Figure 1. (**a**) Structural representation of the ferrihydrite f-phase in projection along the $[\bar{1}\bar{1}0]$ axis and in perspective to show the polyhedral associations. Adapted from Manceau et al. (2011). (**b** and **c**) Akdalaite model (Michel et al., 2007), and modified akdalaite model which is structurally analogue to the 2x2x1 supercell of the f-phase (Manceau and Gates, 2013; Paktunc et al., 2013). The akdalaite model is composed of O,OH sheets closely-packed with ABACA stacking, and Fe atoms in both octahedral (80% of Fe sites) and tetrahedral (20% of Fe sites) coordination. The f-phase has the same anionic packing, but a different proportion and distribution of O and OH, and 100% of the Fe atoms are octahedral occupying 50% of the octahedral sites in each anion layer (Drits et al., 1993). Distribution of Fe across the anion layers is such that there are no face-sharing arrangements between Fe octahedra along the B and C planes of the structure and that hydroxyls are confined to the A and oxygen to the B and C layers. (**b**) Structure refined from the 6Fh PDF with nineteen parameters (Supplementary Table S3).

Figure 2 Experimental XRD patterns for six-line (Manceau, 2009) and seven-line (Berquo et al., 2007) ferrihydrite, and calculated XRD pattern for the fhyd6 variant of the akdalaite model (Michel et al., 2007).

Figure 3 (**a**) Experimental PDF for six-line ferrihydrite (fhyd6) and refined fit of the akdalaite model reproduced from Figure 2a of Michel et al. (2007). (**b**) Experimental PDF for 6Fh and refined fit of the akdalaite model. (**c**) Comparison of the best-fit PDFs obtained with the akdalaite model (Fig. 1b) and the modified akdalaite model (Fig. 1c).

Figure 4 Overlay plots of the experimental PDFs for three phyllomanganates having different layer stacking order (Zhu et al., 2012; Manceau et al., 2013). K-birnessite (KBi8) is *c*-ordered with few stacking faults; δ-MnO_2 has turbostratic disorder, and AcidBir has intermediate stacking disorder. KBi8 and AcidBir have nearly the same structural formula, hence a similar short-range layer structure. The severe decrease of the peaks amplitude beyond 7.2 Å is caused by stacking faults which make unequal the layer-to-layer pair distances. Similar effect is observed in ferrihydrite beyond 4.5 Å.

Figure 5 Near-neighbor PDF peaks for six-line ferrihydrite (6Fh) and K-birnessite (KBi8) (Gaillot et al., 2003; Manceau et al., 2013). The difference of average Fe-O (~1.99 Å) and Mn-O (~1.91 Å) distances between the two materials was offset by shifting the KBi8 PDF by +0.085 Å. When aligned, the two peaks appear symmetrical, which argues against the presence of tetrahedral Fe in 6Fh.

Table 1. Calculated bond valence sums for three models of the ferrihydrite PDF. The values in bold are unrealistic.

Atom	Type	Akdalaite model - fhyd6[a]	Akdalaite model – ferrifh[b]	Akdalaite model – this study[c]	Akdalaite model – this study[d]	Modified akdalaite model – this study[e]
O1	OH	**1.87**	0.94	**2.11**	**2.29**	0.76
O2	O	2.32	1.89	2.45	2.46	1.69
O3	O	1.74	1.91	1.77	1.76	1.75-1.82
O4	O	1.88	2.28	1.80	1.78	1.18-1.24
Fe1	Fe^{3+}	2.82	2.97	2.86	2.95	2.39
Fe2	Fe^{3+}	**3.92**	2.97	**3.90**	**3.67**	**3.79**
Fe3	Fe^{3+}	2.70	2.74	2.81	2.88	2.79

[a] From Michel et al. (2007) with ^{VI}Fe and ^{IV}Fe and 20 parameters adjusted. [b] From Michel et al. (2010) with ^{VI}Fe and ^{IV}Fe and 19 parameters adjusted. [c] This study, with ^{VI}Fe and ^{IV}Fe and 20 parameters adjusted (Supplementary Table 1). [d] This study with ^{VI}Fe and ^{IV}Fe and 19 parameters adjusted (Supplementary Table 2). [e] This study with ^{VI}Fe only and 19 parameters adjusted.

Table 2. Evaluation of the distortion of the Fe polyhedra in the different akdalaite models and akaganeite (β-FeOOH). Values in bold indicate strong distortion.

		Δ (Å)[a]	Volume eccentricity[b]
Akdalaite model - fhyd6 – Michel et al. (2007)	^{VI}Fe1	0.103	0.144
	^{VI}Fe2	0.082	0.123
	^{IV}Fe3	0.155	0.221
Akdalaite model – ferrifh – Michel et al. (2010)	^{VI}Fe1	0.096	0.136
	^{VI}Fe2	**0.285**	**0.363**
	^{IV}Fe3	0.090	0.136
Akdalaite model – this study[c]	^{VI}Fe1	0.127	0.175
	^{VI}Fe2	0.141	0.205
	^{IV}Fe3	0.120	0.177
Akdalaite model – this study[d]	^{VI}Fe1	0.143	0.195
	^{VI}Fe2	0.111	0.162
	^{IV}Fe3	**0.275**	**0.364**
Modified akdalaite model – this study	^{VI}Fe1	0.179	0.234
	^{VI}Fe2	0.080	0.120
	^{VI}Fe3	**0.227**	**0.297**
Akaganeite – (Post et al., 2003)	^{VI}Fe1	0.112	0.159
	^{VI}Fe2	0.113	0.158

[a] Distance of the central atom to the centroid. [b] volume eccentricity calculated as $1 - [(r_s - \Delta)/r_s]^3$ with r_s the average distance from the centroid to the ligands. [c] This study, 20 parameters adjusted (Supplementary Table 1). [d] This study, 19 parameters adjusted (Supplementary Table 2).

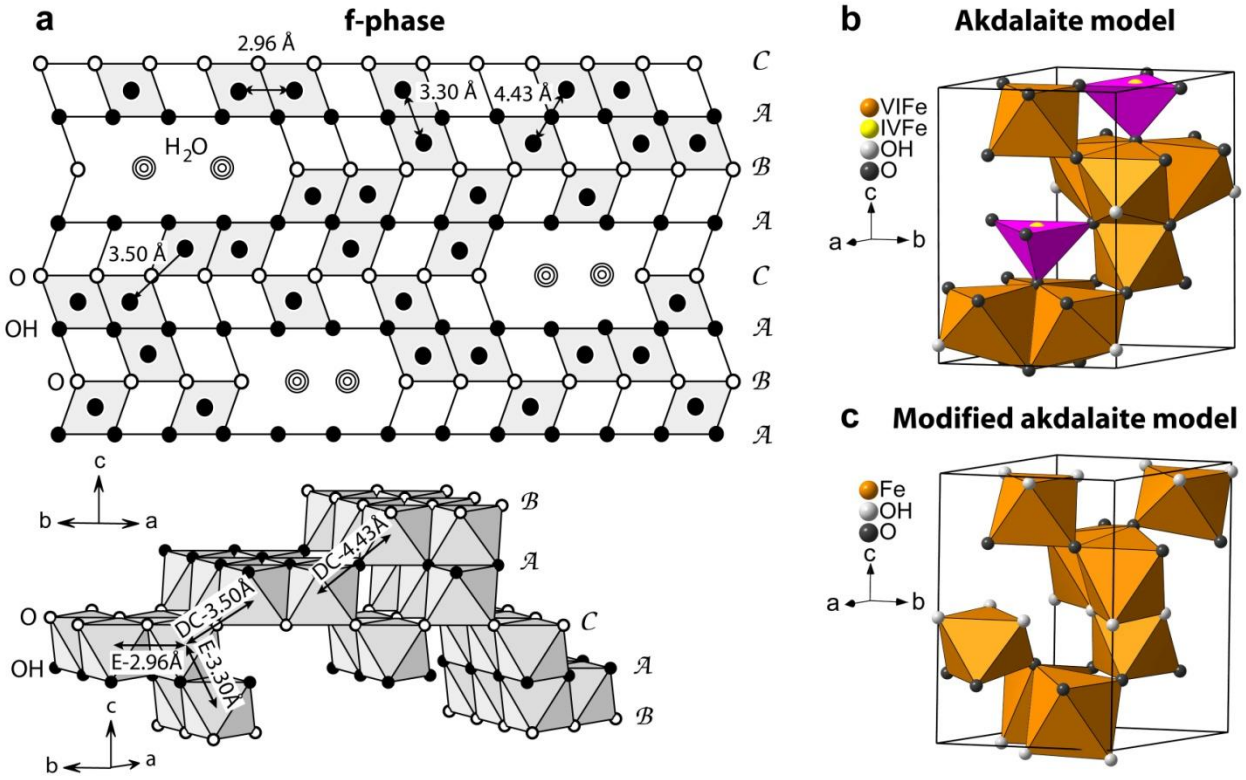

Figure 1

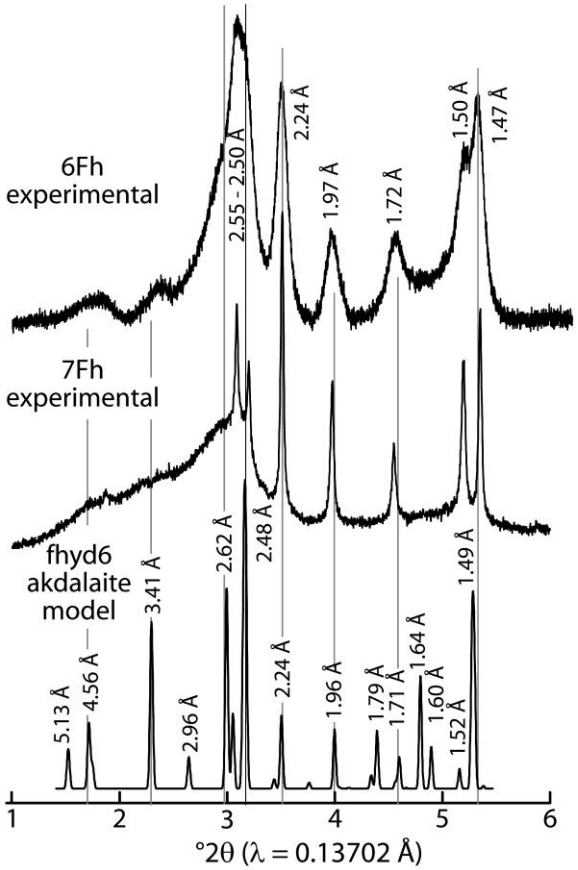

Figure 2

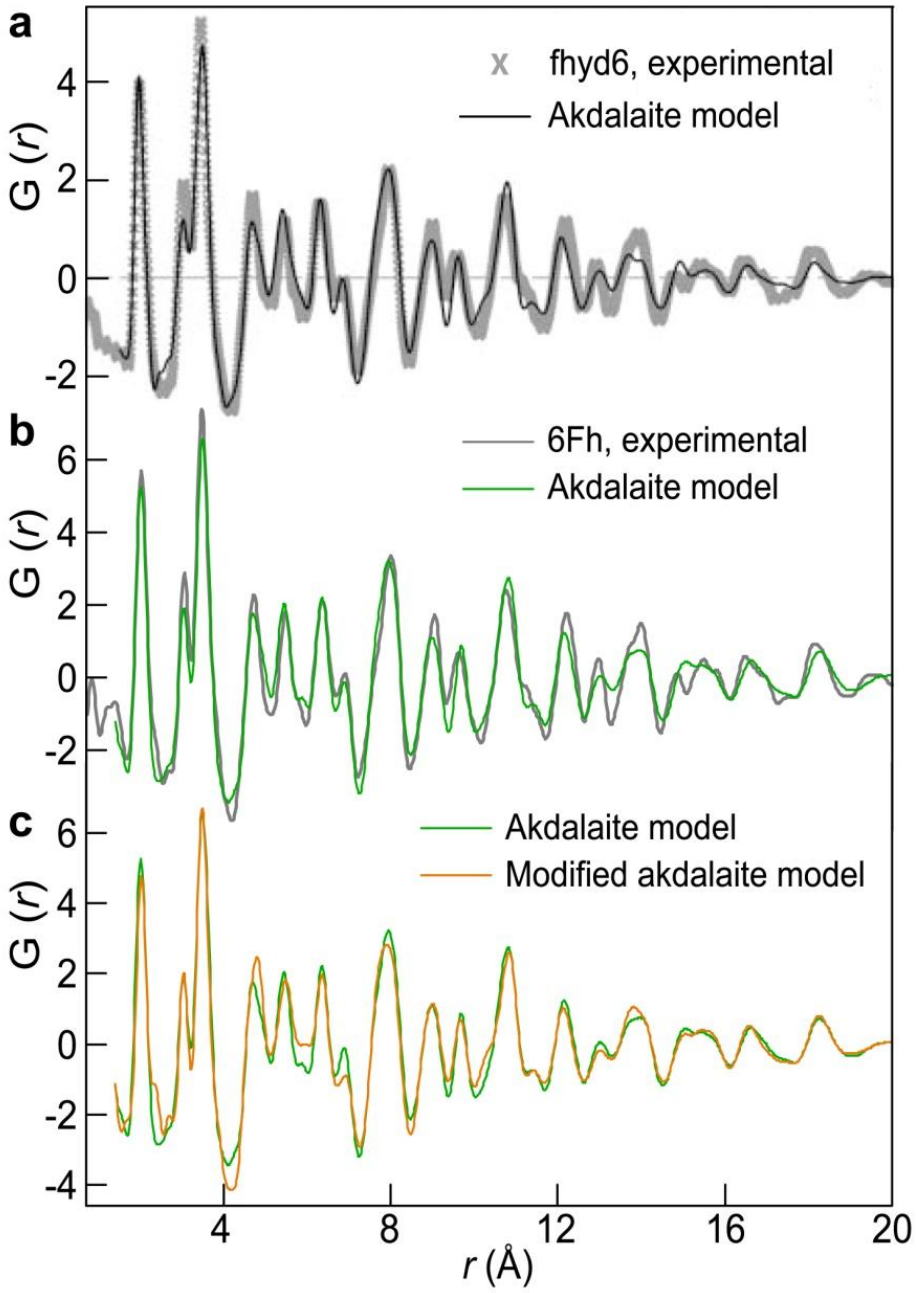
a
fhyd6, experimental
Akdalaite model
G (r)
b
6Fh, experimental
Akdalaite model
c
Akdalaite model
Modified akdalaite model
r (Å)

Figure 3

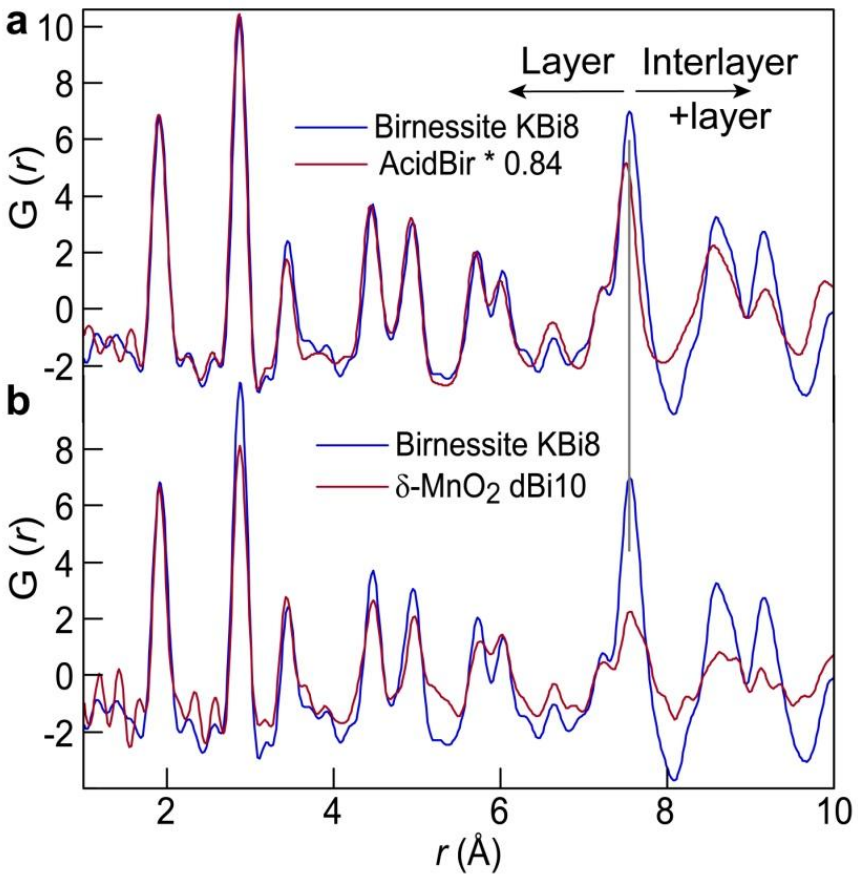

Figure 4

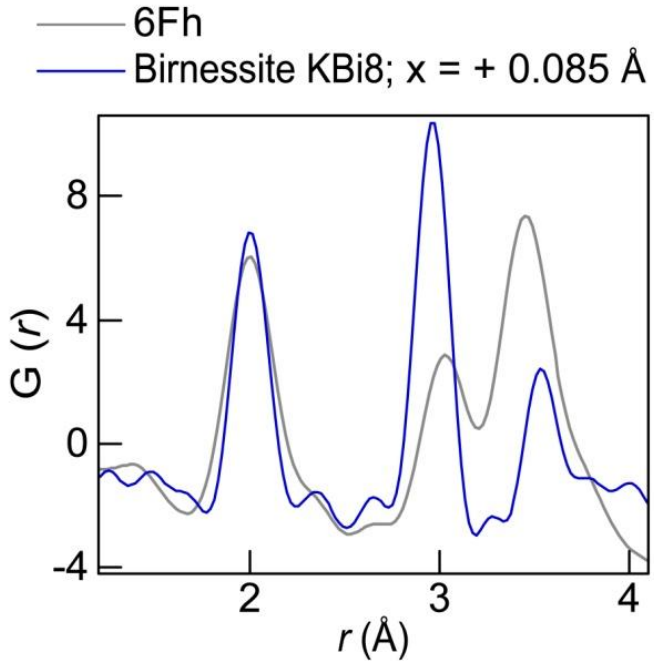

Figure 5

Supplement for the article: PDF analysis of ferrihydrite: Critical assessment of the underconstrained akdalaite model

Figure S1. Structure of the akdalaite model and its parametrization in PDFgui

Polyhedral representation of the akdalaite unit cell. Independent atoms in the asymmetric unit are labeled.

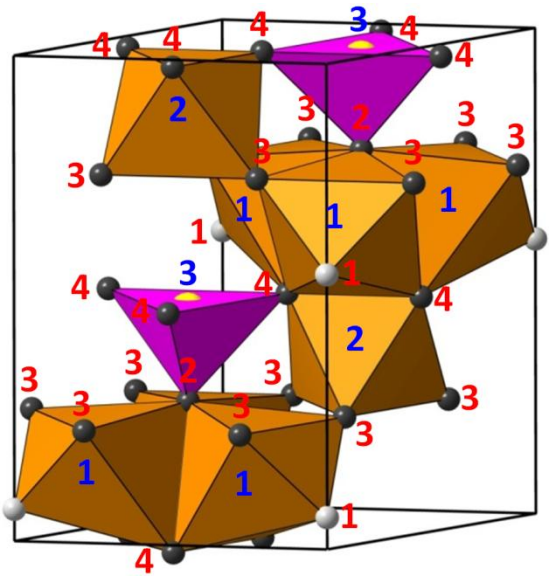

Screen shot of the PDFgui interface window showing the parametrization of the akdalaite model. Symmetry-related positions in the full cell were generated from the asymmetric unit and symmetry constraints of the *P*6$_3$*mc* space group.

Phase Constraints

a @4 b @4 c @5
alpha beta gamma

Scale Factor
delta1 @6 delta2 spdiameter @8
sratio

Included Pairs all-all

	elem	x	y	z	u11	u22	u33	u12	u13	u23	occ
1	Fe 1	@11	-@11 +1	@12	@100	@100	@100				@301
2	Fe 1	@11	+2*@11	@12	@100	@100	@100				@301
3	Fe 1	-2*@11 +1	-@11 +1	@12	@100	@100	@100				@301
4	Fe 1	-@11 +1	@11	@12 -0.5	@100	@100	@100				@301
5	Fe 1	-@11 +1	-2*@11 +1	@12 -0.5	@100	@100	@100				@301
6	Fe 1	+2*@11	@11	@12 -0.5	@100	@100	@100				@301
7	Fe 2			@13	@100	@100	@100				@302
8	Fe 2			@13 +0.5	@100	@100	@100				@302
9	Fe 3			@15	@100	@100	@100				@303
10	Fe 3			@15 -0.5	@100	@100	@100				@303
11	O 1			@16	@200	@200	@200				
12	O 1			@16 +0.5	@200	@200	@200				
13	O 2			@17	@200	@200	@200				
14	O 2			@17 +0.5	@200	@200	@200				
15	O 3	@18	-@18 +1	@19	@200	@200	@200				
16	O 3	@18	+2*@18	@19	@200	@200	@200				
17	O 3	-2*@18 +1	-@18 +1	@19	@200	@200	@200				
18	O 3	-@18 +1	@18	@19 +0.5	@200	@200	@200				
19	O 3	-@18 +1	-2*@18 +1	@19 +0.5	@200	@200	@200				
20	O 3	+2*@18	@18	@19 +0.5	@200	@200	@200				
21	O 4	@20	-@20 +1	@21	@200	@200	@200				
22	O 4	@20	+2*@20 -1	@21	@200	@200	@200				
23	O 4	-2*@20 +2	-@20 +1	@21	@200	@200	@200				
24	O 4	-@20 +1	@20	@21 -0.5	@200	@200	@200				
25	O 4	-@20 +1	-2*@20 +2	@21 -0.5	@200	@200	@200				
26	O 4	+2*@20 -1	@20	@21 -0.5	@200	@200	@200				

Screen shot of the initial and refined parameter values. The Fe1 site occupancy was fixed to 1.0 to reduce correlations (19 parameters adjusted).

	Initial	Fixed	Refined
@ 1	1.3	☐	1.26078215171
@ 2	0.137	☐	0.0735800893587
@ 4	5.928	☐	5.94375215241
@ 5	9.126	☐	9.16963651216
@ 6	1.8	☐	1.88517177714
@ 8	35.0	☑	35.0
@ 11	0.1695	☐	0.16918043634
@ 12	0.6365	☐	0.63630493601
@ 13	0.3379	☐	0.331055495526
@ 15	0.9595	☐	0.953356338802
@ 16	0.0446	☐	0.0659270295649
@ 17	0.7634	☐	0.769203681119
@ 18	0.1697	☐	0.167758743399
@ 19	0.2467	☐	0.244748555132
@ 20	0.5227	☐	0.523994536215
@ 21	0.9796	☐	0.980284557646
@100	0.011	☐	0.0117534396498
@200	0.007	☐	0.00384039869658
@301	1.0	☑	1.0
@302	0.97	☐	0.855348533147
@303	0.96	☐	0.861677349147

@1 is the scale factor and @2 is the resolution dampening (Q_{damp}). Q_{broad} was fixed to 0.069 Å^{-1}. Full results are listed in Table S2.

Figure S2. Structure of the modified akdalaite model and its parametrization in PDFgui

Polyhedral representation of the modified akdalaite unit cell. Independent atoms in the asymmetric unit are labeled. The oxgen atoms and hydroxyls are positioned as in the f-phase (Fig. 1).

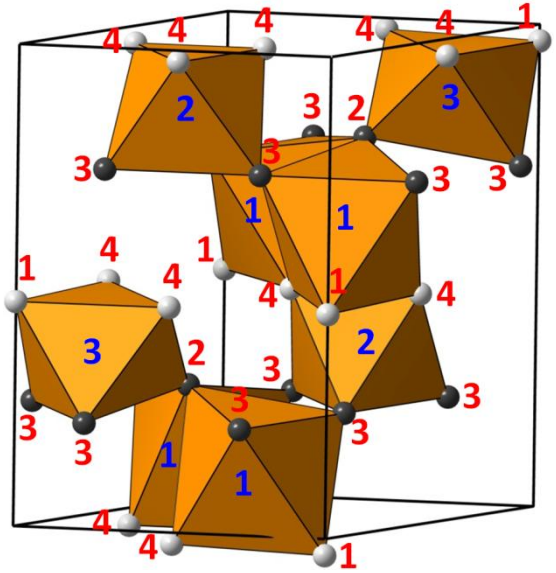

Screen shot of the PDFgui interface window showing the parametrization of the modified akdalaite model.

Phase Constraints

a @4 b @4 c @5
alpha beta gamma

Scale Factor
delta1 delta2 spdiameter @8
sratio @6

Included Pairs all-all

	elem	x	y	z	u11	u22	u33	u12	u13	u23	occ
1	Fe 1	@11	+2*@11	@12	@100	@100	@100				@301
2	Fe 1	-2*@11 +1	-@11 +1	@12	@100	@100	@100				@301
3	Fe 1	-@11 +1	-2*@11 +1	@12 -0.5	@100	@100	@100				@301
4	Fe 1	+2*@11	@11	@12 -0.5	@100	@100	@100				@301
5	Fe 2			@13	@100	@100	@100				@302
6	Fe 2			@13 +0.5	@100	@100	@100				@302
7	Fe 3	@14	-@14 +1	@15	@100	@100	@100				@303
8	Fe 3	-@14 +1	@14	@15 -0.5	@100	@100	@100				@303
9	O 1			@16	@200	@200	@200				
10	O 1			@16 +0.5	@200	@200	@200				
11	O 2			@17	@200	@200	@200				
12	O 2			@17 +0.5	@200	@200	@200				
13	O 3	@18	-@18 +1	@19	@200	@200	@200				
14	O 3	@18	+2*@18	@19	@200	@200	@200				
15	O 3	-2*@18 +1	-@18 +1	@19	@200	@200	@200				
16	O 3	-@18 +1	@18	@19 +0.5	@200	@200	@200				
17	O 3	-@18 +1	-2*@18 +1	@19 +0.5	@200	@200	@200				
18	O 3	+2*@18	@18	@19 +0.5	@200	@200	@200				
19	O 4	@20	-@20 +1	@21	@200	@200	@200				
20	O 4	@20	+2*@20 -1	@21	@200	@200	@200				
21	O 4	-2*@20 +2	-@20 +1	@21	@200	@200	@200				
22	O 4	-@20 +1	@20	@21 -0.5	@200	@200	@200				
23	O 4	-@20 +1	-2*@20 +2	@21 -0.5	@200	@200	@200				
24	O 4	+2*@20 -1	@20	@21 -0.5	@200	@200	@200				

Screen shot of the initial and refined parameter values.

		Initial	Fixed	Refined
@	1	1.3	☐	1.46023322482
@	2	0.137	☐	0.0797513125045
@	4	5.928	☐	5.95041595549
@	5	9.126	☐	9.13279706467
@	6	1.0	☐	0.461806863636
@	8	35.0	☑	35.0
@	11	0.1695	☐	0.17491586752
@	12	0.6365	☑	0.6365
@	13	0.3379	☐	0.320720779344
@	14	0.1697	☐	0.169786935837
@	15	0.85	☐	0.842817540034
@	16	-0.0446	☐	-0.0344265657565
@	17	0.7634	☐	0.779493448447
@	18	0.1697	☐	0.167311652982
@	19	0.2467	☐	0.233612214827
@	20	0.5227	☐	0.528761606496
@	21	0.9796	☐	0.971194873621
@	100	0.011	☐	0.00697294046269
@	200	0.007	☐	0.00563328878938
@	301	1.0	☑	1.0
@	302	0.97	☐	1.05785376365
@	303	0.96	☐	0.83144015261

The z(Fe1) position was fixed during the refinement to the value of Michel et al. (2007) to limit the total number of fitted parameters to 19. Full results are listed in Table S3.

Table S1. Results from the akdalaite fit to the 6Fh PDF with 20 adjusted parameters.

```
* Mon Mar 25 09:17:47 2013

==============================================================================
PDF REFINEMENT
  Using PDFFIT version : 1.0-r6773-20111122
==============================================================================
------------------------------------------------------------------------------
PHASE 1 : UNNAMED
------------------------------------------------------------------------------
Scale factor           : 1
  Particle diameter    : 35 A
  Step cutoff          : not applied
Quad. corr. factor     : 0
Lin. corr. factor      : 1.81458 (0.21)
Low r sigma ratio      : 1
R cutoff [A]           : 0
Lattice parameters     : 5.9395 (0.0092)     5.9395 (0.0092)     9.17173 (0.025)
          & angles     : 90                  90                  120

Atom positions & occupancies :
  FE    0.170377 (0.001)    0.829623 (0.001)    0.638305 (2.2e+04)  0.82616 (0.076)
  FE    0.170377 (0.001)    0.340754 (0.002)    0.638305 (2.2e+04)  0.82616 (0.076)
  FE    0.659246 (0.002)    0.829623 (0.001)    0.638305 (2.2e+04)  0.82616 (0.076)
  FE    0.829623 (0.001)    0.170377 (0.001)    0.138305 (2.2e+04)  0.82616 (0.076)
  FE    0.829623 (0.001)    0.659246 (0.002)    0.138305 (2.2e+04)  0.82616 (0.076)
  FE    0.340754 (0.002)    0.170377 (0.001)    0.138305 (2.2e+04)  0.82616 (0.076)
  FE    0.333333            0.666667            0.334625 (2.2e+04)  0.736728 (0.18)
  FE    0.666667            0.333333            0.834625 (2.2e+04)  0.736728 (0.18)
  FE    0.333333            0.666667            0.953882 (2.2e+04)  0.815759 (0.14)
  FE    0.666667            0.333333            0.453882 (2.2e+04)  0.815759 (0.14)
  O     0                   0                   0.0612022 (2.2e+04) 1
  O     0                   0                   0.561202 (2.2e+04)  1
  O     0.333333            0.666667            0.757992 (2.2e+04)  1
  O     0.666667            0.333333            0.257992 (2.2e+04)  1
  O     0.171725 (0.0041)   0.828275 (0.0041)   0.246359 (2.2e+04)  1
  O     0.171725 (0.0041)   0.343449 (0.0082)   0.246359 (2.2e+04)  1
  O     0.656551 (0.0082)   0.828275 (0.0041)   0.246359 (2.2e+04)  1
  O     0.828275 (0.0041)   0.171725 (0.0041)   0.746359 (2.2e+04)  1
  O     0.828275 (0.0041)   0.656551 (0.0082)   0.746359 (2.2e+04)  1
  O     0.343449 (0.0082)   0.171725 (0.0041)   0.746359 (2.2e+04)  1
  O     0.519454 (0.0035)   0.480546 (0.0035)   0.977773 (2.2e+04)  1
  O     0.519454 (0.0035)   0.0389082 (0.0071)  0.977773 (2.2e+04)  1
  O     0.961092 (0.0071)   0.480546 (0.0035)   0.977773 (2.2e+04)  1
  O     0.480546 (0.0035)   0.519454 (0.0035)   0.477773 (2.2e+04)  1
  O     0.480546 (0.0035)   0.961092 (0.0071)   0.477773 (2.2e+04)  1
  O     0.0389082 (0.0071)  0.519454 (0.0035)   0.477773 (2.2e+04)  1

Anisotropic temperature factors :
  FE    0.0105771 (0.0011)  0.0105771 (0.0011)  0.0105771 (0.0011)
  FE    0.0105771 (0.0011)  0.0105771 (0.0011)  0.0105771 (0.0011)
  FE    0.0105771 (0.0011)  0.0105771 (0.0011)  0.0105771 (0.0011)
  FE    0.0105771 (0.0011)  0.0105771 (0.0011)  0.0105771 (0.0011)
  FE    0.0105771 (0.0011)  0.0105771 (0.0011)  0.0105771 (0.0011)
  FE    0.0105771 (0.0011)  0.0105771 (0.0011)  0.0105771 (0.0011)
  FE    0.0105771 (0.0011)  0.0105771 (0.0011)  0.0105771 (0.0011)
  FE    0.0105771 (0.0011)  0.0105771 (0.0011)  0.0105771 (0.0011)
  FE    0.0105771 (0.0011)  0.0105771 (0.0011)  0.0105771 (0.0011)
  FE    0.0105771 (0.0011)  0.0105771 (0.0011)  0.0105771 (0.0011)
  O     0.0105045 (0.0024)  0.0105045 (0.0024)  0.0105045 (0.0024)
  O     0.0105045 (0.0024)  0.0105045 (0.0024)  0.0105045 (0.0024)
  O     0.0105045 (0.0024)  0.0105045 (0.0024)  0.0105045 (0.0024)
  O     0.0105045 (0.0024)  0.0105045 (0.0024)  0.0105045 (0.0024)
  O     0.0105045 (0.0024)  0.0105045 (0.0024)  0.0105045 (0.0024)
  O     0.0105045 (0.0024)  0.0105045 (0.0024)  0.0105045 (0.0024)
  O     0.0105045 (0.0024)  0.0105045 (0.0024)  0.0105045 (0.0024)
  O     0.0105045 (0.0024)  0.0105045 (0.0024)  0.0105045 (0.0024)
  O     0.0105045 (0.0024)  0.0105045 (0.0024)  0.0105045 (0.0024)
  O     0.0105045 (0.0024)  0.0105045 (0.0024)  0.0105045 (0.0024)
  O     0.0105045 (0.0024)  0.0105045 (0.0024)  0.0105045 (0.0024)
  O     0.0105045 (0.0024)  0.0105045 (0.0024)  0.0105045 (0.0024)
  O     0.0105045 (0.0024)  0.0105045 (0.0024)  0.0105045 (0.0024)
  O     0.0105045 (0.0024)  0.0105045 (0.0024)  0.0105045 (0.0024)
  O     0.0105045 (0.0024)  0.0105045 (0.0024)  0.0105045 (0.0024)
  O     0.0105045 (0.0024)  0.0105045 (0.0024)  0.0105045 (0.0024)
```

```
--------------------------------------------------------------------------------
DATA SET : 1 (string)
--------------------------------------------------------------------------------
Data range in r [A]     : 1.38     -> 20            Step dr   : 0.02
Calculated range        : 1.38     -> 21.7952
Refinement r range      : 1.38     -> 20            Data pts : 0     -> 931
Reduced chi squared     : 0.222497
Rw - value              : 0.297642


Experimental settings  :
  Radiation             : X-Rays
  Termination at Qmax   : 21 A**-1
  DQ dampening Qdamp    : 0.0727986 (0.007) A**-1
  DQ broadening Qbroad  : 0.069 A**-1
  Scale factor          : 1.37253 (0.089)

Selected phases and atoms for this data set :
  Phase 1 :
    Atoms (i) :  FE  O
    Atoms (j) :  FE  O

Relative phase content in terms of
          atoms                   unit cells              mass
Phase 1 : 1                       1                       1

--------------------------------------------------------------------------------
PARAMETER INFORMATION :
--------------------------------------------------------------------------------
Number of constraints        : 157
Number of refined parameters : 20
Number of fixed parameters   : 1

Refinement parameters :
  1: 1.37253 (0.089)         2: 0.0727986 (0.007)       4: 5.9395 (0.0092)
  5: 9.17173 (0.025)         6: 1.81458 (0.21)          8: 35
 11: 0.170377 (0.001)       12: 0.638305 (2.2e+04)     13: 0.334625 (2.2e+04)
 15: 0.953882 (2.2e+04)     16: 0.0612022 (2.2e+04)    17: 0.757992 (2.2e+04)
 18: 0.171725 (0.0041)      19: 0.246359 (2.2e+04)     20: 0.519454 (0.0035)
 21: 0.977773 (2.2e+04)    100: 0.0105771 (0.0011)    200: 0.0105045 (0.0024)
301: 0.82616 (0.076)       302: 0.736728 (0.18)       303: 0.815759 (0.14)
--------------------------------------------------------------------------------
REFINEMENT INFORMATION:
--------------------------------------------------------------------------------
Number of iterations : 5
Reduced chi squared  : 0.204832
Rw - value           : 0.285582

Correlations greater than 0.8 :

  Corr(p[12], p[13]) = 1
  Corr(p[12], p[15]) = 1
  Corr(p[12], p[16]) = 1
  Corr(p[12], p[17]) = 1
  Corr(p[12], p[19]) = 1
  Corr(p[12], p[21]) = 1
  Corr(p[13], p[15]) = 1
  Corr(p[13], p[16]) = 1
  Corr(p[13], p[17]) = 1
  Corr(p[13], p[19]) = 1
  Corr(p[13], p[21]) = 1
  Corr(p[15], p[16]) = 1
  Corr(p[15], p[17]) = 1
  Corr(p[15], p[19]) = 1
  Corr(p[15], p[21]) = 1
  Corr(p[16], p[17]) = 1
  Corr(p[16], p[19]) = 1
  Corr(p[16], p[21]) = 1
  Corr(p[17], p[19]) = 1
  Corr(p[17], p[21]) = 1
  Corr(p[19], p[21]) = 1
  Corr(p[302], p[303]) = -0.823727
================================================================================
```

Table S2. Results from the akdalaite fit to the 6Fh PDF with 19 adjusted parameters

```
* Mon Mar 25 09:19:53 2013

 ==============================================================================
 PDF REFINEMENT
   Using PDFFIT version : 1.0-r6773-20111122
 ==============================================================================
 ------------------------------------------------------------------------------
 PHASE 1 : UNNAMED
 ------------------------------------------------------------------------------
 Scale factor          : 1
   Particle diameter   : 35 A
   Step cutoff         : not applied
 Quad. corr. factor    : 0
 Lin. corr. factor     : 1.88517 (0.0072)
 Low r sigma ratio     : 1
 R cutoff [A]          : 0
 Lattice parameters    : 5.94375 (0.0083)    5.94375 (0.0083)    9.16964 (0.023)
           & angles    : 90                  90                  120

 Atom positions & occupancies :
   FE    0.16918 (0.0011)    0.83082 (0.0011)    0.636305          1
   FE    0.16918 (0.0011)    0.338361 (0.0022)   0.636305          1
   FE    0.661639 (0.0022)   0.83082 (0.0011)    0.636305          1
   FE    0.83082 (0.0011)    0.16918 (0.0011)    0.136305          1
   FE    0.83082 (0.0011)    0.661639 (0.0022)   0.136305          1
   FE    0.338361 (0.0022)   0.16918 (0.0011)    0.136305          1
   FE    0.333333            0.666667            0.331055          0.855349 (0.2)
   FE    0.666667            0.333333            0.831055          0.855349 (0.2)
   FE    0.333333            0.666667            0.953356          0.861677 (0.15)
   FE    0.666667            0.333333            0.453356          0.861677 (0.15)
   O     0                   0                   0.065927          1
   O     0                   0                   0.565927          1
   O     0.333333            0.666667            0.769204          1
   O     0.666667            0.333333            0.269204          1
   O     0.167759 (0.0027)   0.832241 (0.0027)   0.244749          1
   O     0.167759 (0.0027)   0.335517 (0.0055)   0.244749          1
   O     0.664483 (0.0055)   0.832241 (0.0027)   0.244749          1
   O     0.832241 (0.0027)   0.167759 (0.0027)   0.744749          1
   O     0.832241 (0.0027)   0.664483 (0.0055)   0.744749          1
   O     0.335517 (0.0055)   0.167759 (0.0027)   0.744749          1
   O     0.523995 (0.003)    0.476005 (0.003)    0.980285          1
   O     0.523995 (0.003)    0.0479891 (0.0059)  0.980285          1
   O     0.952011 (0.0059)   0.476005 (0.003)    0.980285          1
   O     0.476005 (0.003)    0.523995 (0.003)    0.480285          1
   O     0.476005 (0.003)    0.952011 (0.0059)   0.480285          1
   O     0.0479891 (0.0059)  0.523995 (0.003)    0.480285          1

 Anisotropic temperature factors :
   FE    0.0117534 (0.0011)  0.0117534 (0.0011)  0.0117534 (0.0011)
   FE    0.0117534 (0.0011)  0.0117534 (0.0011)  0.0117534 (0.0011)
   FE    0.0117534 (0.0011)  0.0117534 (0.0011)  0.0117534 (0.0011)
   FE    0.0117534 (0.0011)  0.0117534 (0.0011)  0.0117534 (0.0011)
   FE    0.0117534 (0.0011)  0.0117534 (0.0011)  0.0117534 (0.0011)
   FE    0.0117534 (0.0011)  0.0117534 (0.0011)  0.0117534 (0.0011)
   FE    0.0117534 (0.0011)  0.0117534 (0.0011)  0.0117534 (0.0011)
   FE    0.0117534 (0.0011)  0.0117534 (0.0011)  0.0117534 (0.0011)
   FE    0.0117534 (0.0011)  0.0117534 (0.0011)  0.0117534 (0.0011)
   FE    0.0117534 (0.0011)  0.0117534 (0.0011)  0.0117534 (0.0011)
   O     0.0038404 (0.0016)  0.0038404 (0.0016)  0.0038404 (0.0016)
   O     0.0038404 (0.0016)  0.0038404 (0.0016)  0.0038404 (0.0016)
   O     0.0038404 (0.0016)  0.0038404 (0.0016)  0.0038404 (0.0016)
   O     0.0038404 (0.0016)  0.0038404 (0.0016)  0.0038404 (0.0016)
   O     0.0038404 (0.0016)  0.0038404 (0.0016)  0.0038404 (0.0016)
   O     0.0038404 (0.0016)  0.0038404 (0.0016)  0.0038404 (0.0016)
   O     0.0038404 (0.0016)  0.0038404 (0.0016)  0.0038404 (0.0016)
   O     0.0038404 (0.0016)  0.0038404 (0.0016)  0.0038404 (0.0016)
   O     0.0038404 (0.0016)  0.0038404 (0.0016)  0.0038404 (0.0016)
   O     0.0038404 (0.0016)  0.0038404 (0.0016)  0.0038404 (0.0016)
   O     0.0038404 (0.0016)  0.0038404 (0.0016)  0.0038404 (0.0016)
   O     0.0038404 (0.0016)  0.0038404 (0.0016)  0.0038404 (0.0016)
   O     0.0038404 (0.0016)  0.0038404 (0.0016)  0.0038404 (0.0016)
   O     0.0038404 (0.0016)  0.0038404 (0.0016)  0.0038404 (0.0016)
   O     0.0038404 (0.0016)  0.0038404 (0.0016)  0.0038404 (0.0016)
   O     0.0038404 (0.0016)  0.0038404 (0.0016)  0.0038404 (0.0016)
```

```
--------------------------------------------------------------------------------
DATA SET : 1 (string)
--------------------------------------------------------------------------------
Data range in r [A]     : 1.38     -> 20            Step dr   : 0.02
Calculated range        : 1.38     -> 21.7952
Refinement r range      : 1.38     -> 20            Data pts : 0     -> 931
Reduced chi squared     : 0.183335
Rw - value              : 0.270329


Experimental settings  :
  Radiation             : X-Rays
  Termination at Qmax   : 21 A**-1
  DQ dampening Qdamp    : 0.0735801 (0.0062) A**-1
  DQ broadening Qbroad  : 0.069 A**-1
  Scale factor          : 1.26078 (0.048)

Selected phases and atoms for this data set :
  Phase 1 :
    Atoms (i) :  FE  O
    Atoms (j) :  FE  O

Relative phase content in terms of
          atoms                   unit cells              mass
Phase 1 : 1                       1                       1

--------------------------------------------------------------------------------
PARAMETER INFORMATION :
--------------------------------------------------------------------------------
Number of constraints        : 157
Number of refined parameters : 19
Number of fixed parameters   : 2

Refinement parameters :
  1: 1.26078 (0.048)         2: 0.0735801 (0.0062)      4: 5.94375 (0.0083)
  5: 9.16964 (0.023)         6: 1.88517 (0.0072)        8: 35
 11: 0.16918 (0.0011)       12: 0.636305               13: 0.331055
 15: 0.953356               16: 0.065927               17: 0.769204
 18: 0.167759 (0.0027)      19: 0.244749               20: 0.523995 (0.003)
 21: 0.980285              100: 0.0117534 (0.0011)    200: 0.0038404 (0.0016)
301: 1                     302: 0.855349 (0.2)        303: 0.861677 (0.15)
--------------------------------------------------------------------------------
REFINEMENT INFORMATION:
--------------------------------------------------------------------------------
Number of iterations : 22
Reduced chi squared  : 0.182609
Rw - value           : 0.269793

Correlations greater than 0.8 :

  Corr(p[302], p[303]) = -0.866634
================================================================================
```

Table S3. Results from the modified akdalaite fit to the 6Fh PDF with 19 adjusted parameters

```
* Mon Mar 25 10:00:51 2013

 ==============================================================================
 PDF REFINEMENT
   Using PDFFIT version : 1.0-r6773-20111122
 ==============================================================================
 ------------------------------------------------------------------------------
 PHASE 1 : UNNAMED
 ------------------------------------------------------------------------------
 Scale factor            : 1
   Particle diameter     : 35 A
   Step cutoff           : not applied
 Quad. corr. factor      : 0
 Lin. corr. factor       : 0
 Low r sigma ratio       : 0.461807 (0.1)
 R cutoff [A]            : 4.5
 Lattice parameters      : 5.95042 (0.0071)    5.95042 (0.0071)    9.1328 (0.02)
           & angles      : 90                  90                  120

 Atom positions & occupancies :
   FE    0.174916 (0.00091)  0.349832 (0.0018)   0.6365              1
   FE    0.650168 (0.0018)   0.825084 (0.00091)  0.6365              1
   FE    0.825084 (0.00091)  0.650168 (0.0018)   0.1365              1
   FE    0.349832 (0.0018)   0.174916 (0.00091)  0.1365              1
   FE    0.333333            0.666667            0.320721 (0.0029)   1.05785 (0.13)
   FE    0.666667            0.333333            0.820721 (0.0029)   1.05785 (0.13)
   FE    0.169787 (0.0033)   0.830213 (0.0033)   0.842818 (0.0023)   0.83144 (0.16)
   FE    0.830213 (0.0033)   0.169787 (0.0033)   0.342818 (0.0023)   0.83144 (0.16)
   O     0                   0                   -0.0344266 (0.0046) 1
   O     0                   0                   0.465573 (0.0046)   1
   O     0.333333            0.666667            0.779493 (0.0041)   1
   O     0.666667            0.333333            0.279493 (0.0041)   1
   O     0.167312 (0.0026)   0.832688 (0.0026)   0.233612 (0.0033)   1
   O     0.167312 (0.0026)   0.334623 (0.0051)   0.233612 (0.0033)   1
   O     0.665377 (0.0051)   0.832688 (0.0026)   0.233612 (0.0033)   1
   O     0.832688 (0.0026)   0.167312 (0.0026)   0.733612 (0.0033)   1
   O     0.832688 (0.0026)   0.665377 (0.0051)   0.733612 (0.0033)   1
   O     0.334623 (0.0051)   0.167312 (0.0026)   0.733612 (0.0033)   1
   O     0.528762 (0.0019)   0.471238 (0.0019)   0.971195 (0.0019)   1
   O     0.528762 (0.0019)   0.0575232 (0.0038)  0.971195 (0.0019)   1
   O     0.942477 (0.0038)   0.471238 (0.0019)   0.971195 (0.0019)   1
   O     0.471238 (0.0019)   0.528762 (0.0019)   0.471195 (0.0019)   1
   O     0.471238 (0.0019)   0.942477 (0.0038)   0.471195 (0.0019)   1
   O     0.0575232 (0.0038)  0.528762 (0.0019)   0.471195 (0.0019)   1

 Anisotropic temperature factors :
   FE    0.00697294 (0.00075) 0.00697294 (0.00075) 0.00697294 (0.00075)
   FE    0.00697294 (0.00075) 0.00697294 (0.00075) 0.00697294 (0.00075)
   FE    0.00697294 (0.00075) 0.00697294 (0.00075) 0.00697294 (0.00075)
   FE    0.00697294 (0.00075) 0.00697294 (0.00075) 0.00697294 (0.00075)
   FE    0.00697294 (0.00075) 0.00697294 (0.00075) 0.00697294 (0.00075)
   FE    0.00697294 (0.00075) 0.00697294 (0.00075) 0.00697294 (0.00075)
   FE    0.00697294 (0.00075) 0.00697294 (0.00075) 0.00697294 (0.00075)
   FE    0.00697294 (0.00075) 0.00697294 (0.00075) 0.00697294 (0.00075)
   O     0.00563329 (0.0014) 0.00563329 (0.0014) 0.00563329 (0.0014)
   O     0.00563329 (0.0014) 0.00563329 (0.0014) 0.00563329 (0.0014)
   O     0.00563329 (0.0014) 0.00563329 (0.0014) 0.00563329 (0.0014)
   O     0.00563329 (0.0014) 0.00563329 (0.0014) 0.00563329 (0.0014)
   O     0.00563329 (0.0014) 0.00563329 (0.0014) 0.00563329 (0.0014)
   O     0.00563329 (0.0014) 0.00563329 (0.0014) 0.00563329 (0.0014)
   O     0.00563329 (0.0014) 0.00563329 (0.0014) 0.00563329 (0.0014)
   O     0.00563329 (0.0014) 0.00563329 (0.0014) 0.00563329 (0.0014)
   O     0.00563329 (0.0014) 0.00563329 (0.0014) 0.00563329 (0.0014)
   O     0.00563329 (0.0014) 0.00563329 (0.0014) 0.00563329 (0.0014)
   O     0.00563329 (0.0014) 0.00563329 (0.0014) 0.00563329 (0.0014)
   O     0.00563329 (0.0014) 0.00563329 (0.0014) 0.00563329 (0.0014)
   O     0.00563329 (0.0014) 0.00563329 (0.0014) 0.00563329 (0.0014)
   O     0.00563329 (0.0014) 0.00563329 (0.0014) 0.00563329 (0.0014)
   O     0.00563329 (0.0014) 0.00563329 (0.0014) 0.00563329 (0.0014)
   O     0.00563329 (0.0014) 0.00563329 (0.0014) 0.00563329 (0.0014)
```

```
------------------------------------------------------------------------------
DATA SET : 1 (string)
------------------------------------------------------------------------------
Data range in r [A]     : 1.38     -> 20            Step dr  : 0.02
Calculated range        : 1.38     -> 21.7952
Refinement r range      : 1.38     -> 20            Data pts : 0     -> 931
Reduced chi squared     : 0.270855
Rw - value              : 0.328578


Experimental settings  :
  Radiation             : X-Rays
  Termination at Qmax   : 21 A**-1
  DQ dampening Qdamp    : 0.0797513 (0.0059) A**-1
  DQ broadening Qbroad  : 0.069 A**-1
  Scale factor          : 1.46023 (0.071)

Selected phases and atoms for this data set :
  Phase 1 :
    Atoms (i) :  FE  O
    Atoms (j) :  FE  O

Relative phase content in terms of
          atoms                   unit cells              mass
Phase 1 : 1                       1                       1

------------------------------------------------------------------------------
PARAMETER INFORMATION :
------------------------------------------------------------------------------
Number of constraints        : 147
Number of refined parameters : 19
Number of fixed parameters   : 3

Refinement parameters :
  1: 1.46023 (0.071)         2: 0.0797513 (0.0059)      4: 5.95042 (0.0071)
  5: 9.1328 (0.02)           6: 0.461807 (0.1)          8: 35
 11: 0.174916 (0.00091)     12: 0.6365                 13: 0.320721 (0.0029)
 14: 0.169787 (0.0033)      15: 0.842818 (0.0023)      16: -0.0344266 (0.0046)
 17: 0.779493 (0.0041)      18: 0.167312 (0.0026)      19: 0.233612 (0.0033)
 20: 0.528762 (0.0019)      21: 0.971195 (0.0019)     100: 0.00697294 (0.00075)
200: 0.00563329 (0.0014)   301: 1                      302: 1.05785 (0.13)
303: 0.83144 (0.16)
------------------------------------------------------------------------------
REFINEMENT INFORMATION:
------------------------------------------------------------------------------
Number of iterations : 22
Reduced chi squared  : 0.268319
Rw - value           : 0.327036

Correlations greater than 0.8 :

  *** none ***
==============================================================================
```